

# Effect of annealing on silicon heterojunction solar cells with textured ZnO:Al as transparent conductive oxide

A. Salomon<sup>1,a</sup>, G. Courtois<sup>1,2</sup>, C. Charpentier<sup>1,2</sup>, M. Labrune<sup>1,2</sup>, P. Prod'Homme<sup>1</sup>, L. Francke<sup>1</sup>, and P. Roca i Cabarrocas<sup>2</sup>

<sup>1</sup> TOTAL S.A., Gas & Power – R&D Division, Courbevoie, France

<sup>2</sup> Laboratoire de Physique des Interfaces et des Couches Minces (UMR 7647 CNRS), École Polytechnique, 91128 Palaiseau, France

Received: 26 July 2011 / Accepted: 11 April 2012  
Published online: 12 July 2012

**Abstract** We report on silicon heterojunction solar cells using textured aluminum doped zinc oxide (ZnO:Al) as a transparent conductive oxide (TCO) instead of flat indium tin oxide. Double side silicon heterojunction solar cell were fabricated by radio frequency plasma enhanced chemical vapor deposition on high life time N-type float zone crystalline silicon wafers. On both sides of these cells we have deposited by radio frequency magnetron sputtering ZnO:Al layers of thickness ranging from 800 nm to 1400 nm. These TCO layers were then textured by dipping the samples in a 0.5% hydrochloric acid. External quantum efficiency as well as  $I$ - $V$  under 1 sun illumination measurements showed an increase of the current for the cells using textured ZnO:Al. The cells were then annealed at 150 °C, 175 °C and 200 °C during 30 min in ambient atmosphere and characterized at each annealing step. The results show that annealing has no impact on the open circuit voltage of the devices but that up to a 175 °C it enhances their short circuit current, consistent with an overall enhancement of their spectral response. Our results suggest that ZnO:Al is a promising material to increase the short circuit current ( $J_{sc}$ ) while avoiding texturing the c-Si substrate.

## 1 Introduction

Double side heterojunction (DHJ) solar cells are photovoltaic components with a high potential for making high conversion efficiency and cost effective devices. As a matter of fact the heterojunction with thin intrinsic layer structure developed and industrialized by SANYO reaches efficiencies of 23% [1]. The use of thin amorphous silicon layers for emitter and back surface field (BSF) formation provides high quality surface passivation [2] and high open circuit voltage ( $V_{oc}$ ) [3]. It also makes it possible to manufacture the cells through low temperature processes (200 °C) [4]. Such a low thermal budget allows reducing costs and moreover it allows reducing wafer thickness without breakage [5]. Nevertheless amorphous silicon is more resistive than crystalline silicon, and to ensure good carrier collection it is mandatory to use transparent conductive oxide layer. The one mainly used is indium tin oxide (ITO) because it shows good transmittance (>80%) over the solar spectrum coupled to good conductivity [6,7]. A 75 nm to 80 nm layer of ITO can also be used as an anti-reflective coating (ARC). However ITO suffers from being an expensive material and replacing it by a cheaper TCO is among one of the ways to reduce the costs of DHJ

solar cells [8,9]. Moreover ITO has to be combined with wafer texturing in order to reduce the overall reflectivity of the solar cells as ITO films cannot be textured. It is therefore highly desirable to develop a TCO which could combine antireflection coating properties without needing wafer texturing, as this should help to reduce surface recombination [9,10].

In the past few years aluminum doped zinc oxide (ZnO:Al) has appeared as a good candidate in amorphous and microcrystalline silicon thin film solar cells [11,12]. This material presents good transparency and conductivity properties and it can be textured during or after deposition. But because of its lower conductivity compared to ITO, ( $2 \times 10^{-3} \Omega \text{ cm}$  for ZnO:Al and  $5 \times 10^{-4} \Omega \text{ cm}$  for ITO [8–12]), thick layers (1–2  $\mu\text{m}$ ) are required to achieve low series resistance in the device. Properties of this material can be found elsewhere [13].

To investigate the possibility of using ZnO:Al as a TCO for DHJ silicon solar cells, we fabricated devices with different thicknesses of ZnO:Al on their front and back sides. The TCO material was characterized by Atomic Force Microscopy with an Agilent Technologies 5500. The manufactured cells were characterized by external quantum efficiency (EQE) and current voltage measurements under AM 1.5 using respectively a Cornerstone 260 and Sol3A solar simulator, all of them

<sup>a</sup> e-mail: antoine.salomon@total.com

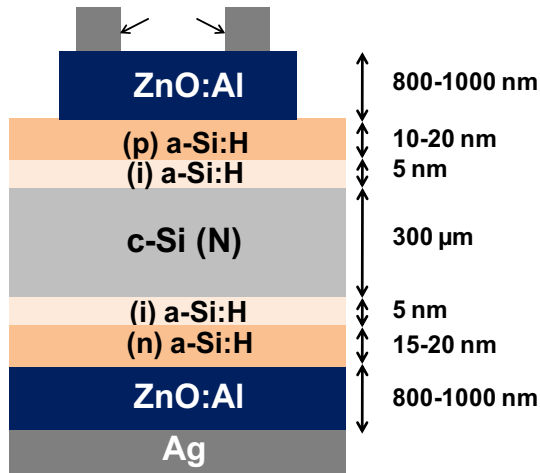


Fig. 1. Schematic of the DHJ.

from Newport Oriel Corporation. We then studied the effect of annealing the samples and characterized them using the same methods as above. Our result show that ZnO:Al could be used as a TCO in DHJ and the texturing of the entire cells by hydrochloric acid (HCl) dip does not alter surface passivation. It also appeared that annealing up to 175 °C increased the current without deteriorating surface passivation. Even though further optimization is still needed for the short circuit current ( $J_{sc}$ ), we could achieve cells with  $V_{oc}$  of 690 mV and fill factor (FF) of 76%.

## 2 Experiments

Figure 1 shows a simple schematic of the DHJ solar cells. Devices are fabricated on n type,  $\langle 100 \rangle$ , 1–5  $\Omega$  cm, float zone silicon wafers. The intrinsic and doped hydrogenated amorphous silicon (a-SiH) layers are deposited at 200 °C by the radio-frequency (13.56 MHz) glow discharge plasma enhanced chemical vapor deposition method in a multiplasma-mono-chamber reactor [14]. Standard intrinsic a-SiH layers are fabricated by the dissociation of pure silane ( $\text{SiH}_4$ ) at a RF power density of 5 mW/cm<sup>2</sup>. P-type (N-type) a-SiH layers were obtained by the dissociation of mixtures of trimethylboron (phosphine), diluted at 1% in  $\text{H}_2$ , and  $\text{SiH}_4$ . For doped layers the RF power density was 5 mW/cm<sup>2</sup>. Before loading the crystalline silicon substrate in the chamber, wafers are dipped in a 5% hydrofluoric acid aqueous solution, to remove the native oxide from its surface. Once the emitter and BSF fabricated, we measured the effective lifetimes by the photo current decay method with a WCT-120 Sinton lifetime tester. The ZnO:Al layers were then deposited by radio frequency magnetron sputtering (13.56 MHz) with argon plasma at 200 °C in an Alliance Concept DP650 system. Finally the front grid is realized by Joule evaporation of silver through a shadow mask, defining a cell area of  $2 \times 2$  cm<sup>2</sup>. The back Ag mirror is done the same way. The thickness of the intrinsic a-Si:H buffer layers, p-doped a-Si:H and n-doped a-Si:H are respectively 5 nm, the 10 nm and 15 nm. The thickness of the ZnO:Al layers ranged from 800 nm to

1.4  $\mu\text{m}$ . For some cells the ZnO:Al electrodes are textured by chemical etching in 0.5% HCl solution [15]. These devices are then annealed at atmospheric pressure under air from 150 °C to 200 °C during 30 min. At each annealing step,  $I$ - $V$  characteristics under 1 sun illumination and spectral responses are measured. The front TCO layer was etched several times in order to reduce its thickness and to increase the scattering properties.

## 3 Results

Figure 2 shows atomic force microscopy (AFM) images of the surface of a ZnO:Al DHJ solar cell after a 20 s dip in a 0.5% HCL aqueous solution. The thickness of ZnO:Al removed during this etch process is of 100 nm on average. The figure shows that the texture produced by HCl chemical attack takes the form of craters. Their diameters are in the interval of 1  $\mu\text{m}$  to 2  $\mu\text{m}$ . The root mean square of the depth is 300 nm. These features show that the surface is rough and thus should improve light scattering in the device. In Figure 3 we present the effect of texturing the ZnO:Al on  $J(V)$  and EQE characteristics. Both samples are prepared with a 1  $\mu\text{m}$  thick ZnO:Al layer on both sides.  $I$ - $V$  curves show that thanks to texturing the current was increased from 14 mA/cm<sup>2</sup> to 18 mA/cm<sup>2</sup>. The  $V_{oc}$  of the devices is unchanged at 690 mV. The fill factor (FF) keeps the same value of 75%. This leads to a 25% increase of the conversion efficiency of the solar cell (from 7% to 9%), when the ZnO:Al layer is textured. Looking at the EQE curves we can see interference fringes for flat ZnO:Al layer which disappear in the textured cell. The impinging light is scattered and thus there is no more privileged optical path. At the same time we observe an improvement of the overall EQE response which is in agreement with the  $J_{sc}$  increase in the  $I$ - $V$  curve. As both samples have the same thickness of ZnO:Al on both sides, this is related to a better scattering and lower reflection of light. The texturation improves the scattering at the back side and reduces reflection at the front side of the solar cell.

In Figure 4 are plotted the EQE and  $I$ - $V$  curves of a sample having a 1  $\mu\text{m}$  thick textured ZnO:Al layer as deposited and then annealed at 150 °C, 175 °C and 200 °C under ambient atmosphere for 30 min. These measurements show an increase of the current as we anneal the samples up to 175 °C and a decrease for higher temperatures.  $I$ - $V$  response under 1 sun shows that the current rises from 17 mA/cm<sup>2</sup> to 21 mA/cm<sup>2</sup> for annealing temperature up to 175 °C and then drops to 19 mA/cm<sup>2</sup>. The same trend is observed for the EQE response. Indeed an improvement of the overall EQE is observed after annealing as compared to the as-deposited state with a maximum spectral response for samples annealed at 175 °C. Upon annealing at 200 °C the response decreases. The maximum of the response is at 600 nm for the as-deposited sample as well as for samples annealed at 150 °C and 175 °C. This maximum shifts to 700 nm following the annealing at 200 °C. It can be explained by the fact that annealing at 200 °C may have made the ZnO:Al layer more dense

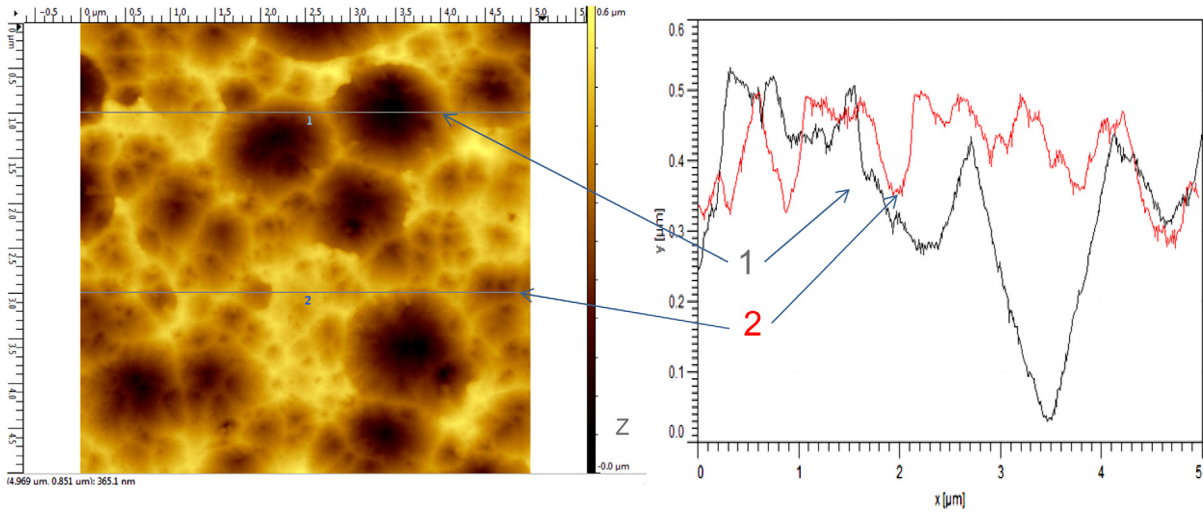


Fig. 2. AFM images of the surface of the ZnO:Al layer after etching 20 s in a 0.5 HCl chemical solution.

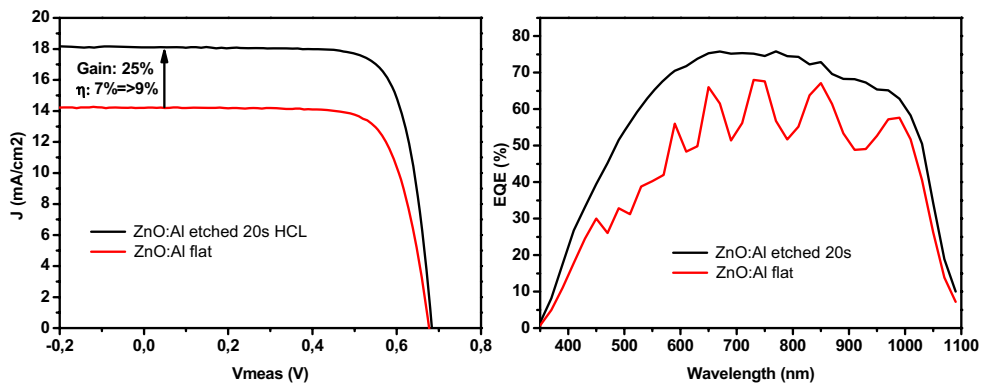


Fig. 3. Comparison of EQE and  $I$ - $V$  under 1 sun illumination of flat and textured ZnO:Al.

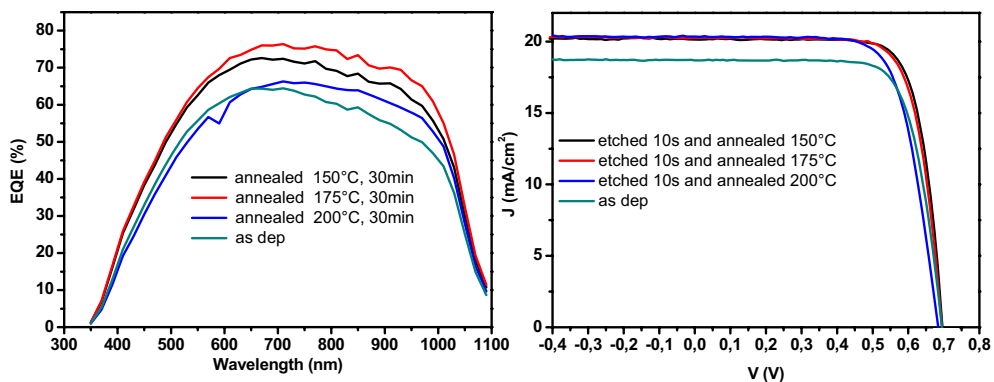
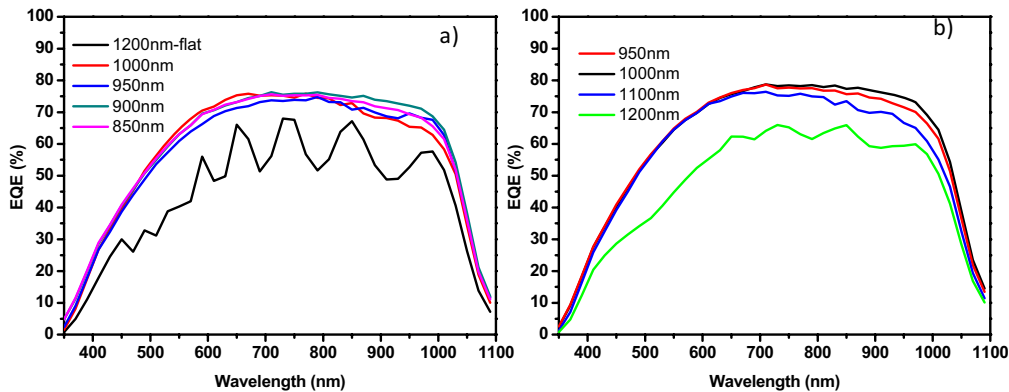


Fig. 4. EQE and  $I$ - $V$  curves of ZnO:Al HJ for different annealing temperature. ZnO:Al thickness: 1  $\mu$ m, annealing 30 min.

and modified its refractive index. When looking at the  $I$ - $V$  characteristics we can notice that annealing does not induce changes in the  $V_{oc}$  which remains at 690 mV, suggesting no losses in surface passivation. The FF encounters small losses. It drops from 76% to 74% as the different annealing steps are done. Despite of this drop of the FF, the conversion efficiency of the cells is improved with annealing because of the increase  $J_{sc}$ . It is of 9% for the

as-deposited cell and goes up to 11% when the sample is annealed at 175 °C.

The effects of successive etching steps of the front ZnO:Al layer by dips in 0.5% HCl solution were studied. Two samples were used during this work. One had a front and back textured ZnO:Al and the other had a front textured ZnO:Al layer with a flat back ZnO:Al one. The back side ZnO:Al is textured by dipping the sample in



**Fig. 5.** EQE curves of HJ for different thickness of textured ZnO:Al layer. (a) Cell with flat back side ZnO:Al. (b) Cell with textured back side ZnO:Al.

a 0.5% HCl before back mirror and front grid deposition. For this sample the front side is also textured. Figure 5 displays the EQE of the samples for different ZnO:Al thickness. In Figure 5a, as in Figure 3, interference fringes are observed for the DHJ initially flat and disappear once the sample is textured. The EQE response of an etched sample is always higher than the one of a flat sample. If EQE of etched samples with different thickness of ZnO:Al are compared, an increase followed by a decrease can be noticed in the infrared (IR) ( $>800$  nm). The response for wavelengths below 700 nm is unaffected by the texturing for thicknesses below 1000 nm. For a thickness or 1000 nm, the response in the UV (500–700 nm) is higher compared to the others. This can be explained by the fact that small features (as can be observed on the AFM images of Fig. 2) diffract more efficiently short wavelengths. The EQE exhibits a maximum for a 950 nm ZnO:Al thickness. In Figure 5b are shown the EQE curves corresponding to the sample with a textured back ZnO:Al side. As observed previously, the EQE increases and the best response is obtained for 1000 nm thick layer. One can also notice, that starting from 1100 nm, reducing the thickness of the ZnO:Al layer by etching does not change the response in the lowest half of the spectra (300 nm to 650 nm) but increases or decreases in the highest second half (650 nm to 1100 nm). If this effect was only related to a change of the absorption because of a thinner ZnO:Al we would expect also to see a change at low wavelength. Therefore we attribute the observed improvement to a better or poorer scattering as well as changes in the ARC properties of the layer.

Finally the influence of texturing of the back ZnO:Al layer was investigated. In Figure 6 are plotted the EQE curves of samples with a front textured ZnO:Al and a back ZnO:Al side that is either flat or textured. For both samples the thickness of the ZnO:Al layers is  $1 \mu\text{m}$ . Both spectra have the same behavior in the interval 350–650 nm. Interestingly, from 650 nm to 1100 nm and most significantly in the region above 800 nm, the EQE response of the sample with a textured back side is above the one of the sample with a flat back side. This shows that part of the IR light is not absorbed by the silicon wafer and

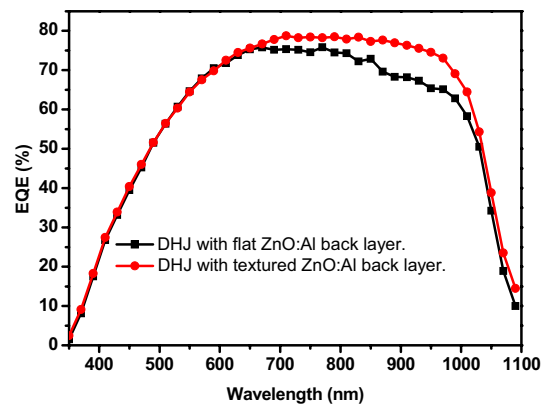


**Fig. 6.** EQE curves of DHJ with flat or textured back side ZnO:Al layer.

that texturing the back side improves its scattering in the sample and thus its absorption.

While our results demonstrate the interest of texturing the ZnO:Al, the EQE responses remain still rather low compared to what can be found in literature for device with ZnO:Al [16, 17]. This may be caused by poor reflectivity as the thickness of the ZnO:Al layer is suited for amorphous PIN and not DHJ. Therefore the next steps will be to optimize the ZnO:Al thickness and the reflectivity in order to further increase the current of the DHJ solar cells.

## 4 Summary and conclusions

We have fabricated DHJ solar cells with ZnO:Al as a front and back electrodes instead of ITO. We have textured this layer after the emitter and BSF deposition by etching in a 0.5% HCl chemical solution. AFM measurements show that the texturing takes the form of craters of  $1 \mu\text{m}$  to  $2 \mu\text{m}$  size and a RMS roughness of 300 nm and that it does not change surface passivation. Thanks to texturing the efficiency of the cells was increased by 25%. We have also studied annealing of DHJ with ZnO:Al.

The thermal treatments were done at 150 °C, 175 °C and 200 °C under air at atmospheric pressure during 30 min. *I-V* under 1 sun illumination measurements showed an increase of 20% of the cell efficiency (from 9% to 11%) for an anneal at 175 °C. Supported by EQE measurements, this was mainly due to an increase of the current generated by the cell. We have studied the influence of the thickness of the ZnO:Al layer by several etch in a 0.5% HCl solution. EQE measurements showed an improvement of the spectral response mainly in the IR region (>800 nm). This can be caused by, on one hand the reduction of the thickness of the front ZnO:Al layer and on another hand by a better diffusion of the light by the texture pattern. Finally we have investigated the texturization of the back side ZnO:Al layer which proved to improve the EQE response in the IR.

The authors would like to thank Jean-François Besnier for the AFM images.

## References

1. T. Mishima, M. Taguchi, H. Sakata, E. Maruyama, *Sol. Energy Mater. Sol. Cells* **95**, 15 (2010)
2. S. Dauwe, J. Schmidt, R. Hezl, *Conference Record of the 29th IEEE*, May 2002, New Orleans, USA
3. H. Sakata, Y. Tsunomura, H. Inoue, S. Taira, T. Baba, H. Kanno, T. Kinoshita, M. Taguchi, E. Maruyama, *Proc. 25th European Photovoltaic Solar Energy Conference and Exhibition Valencia, Spain, 2010*
4. J. Damon-Lacoste, P. Roca i Cabarrocas, P. Chatterjee, Y. Veschetti, A.S. Gudovskikh, J.P. Kleider, P.J. Ribeyron, *J. Non-Cryst. Solids* **352**, 1928 (2006)
5. Y. Tsunomura, Y. Yoshimine, M. Taguchi, T. Baba, T. Kinoshita, H. Kanno, H. Sakata, E. Maruyama, M. Tanaka, *Sol. Energy Mater. Sol. Cells* **93**, 670 (2009)
6. S.-Y. Lien, *Thin Solid Films* **518**, 10 (2010)
7. V.A. Dao, H. Choi, J. Heo, H. Park, K. Yoon, Y. Lee, Y. Kim, N. Lakshminarayan, J. Yi, *Curr. Appl. Phys.* **10**, 5506 (2010)
8. E. Fortunato, D. Ginley, H. Hosono, D.C. Paine, *Mater. Res. Soc. Bull.* **32**, 242 (2007)
9. A. Favier, D. Munõz, S. Martin de Nicolas, P.J. Ribeyron, *Sol. Energy Mater. Sol. Cells* **95**, 1057 (2011)
10. H. Angermann, E. Conrad, L. Korte, J. Rappich, T.F. Schulze, M. Schmidt, *Mater. Sci. Eng. B* **159-160**, 219 (2009)
11. A.G. Aberle, *Thin Solid Films* **517**, 4706 (2009)
12. L.V. Mercaldo, M.L. Addonizio, M. Della Noce, P. Delli Veneri, A. Scognamiglio, C. Privato, *Appl. Energy* **86**, 1836 (2009)
13. C. Charpentier, P. Prod'homme, I. Maurin, M. Chaigneau, P. Roca i Cabarrocas, *Eur. Phys. J Photovolt.* **2**, 25002 (2011)
14. P. Roca i Cabarrocas, J.B. Chévrier, J. Huc, A. Lloret, J.Y. Parey, J.P.M. Schmitt, *J. Vac. Sci. Technol. A* **9**, 2331 (1991)
15. J.I. Owen, J. Hüpkens, H. Zhu, E. Bunte, S.E. Pust, *Phys. Stat. Sol. A* **208**, 109 (2011)
16. O. Kluth, B. Rech, L. Houben, S. Wieder, G. Schöpe, C. Beneking, H. Wagner, A. Löffl, H.W. Schock, *Thin Solid Films* **351**, 247 (1999)
17. J. Müller, B. Rech, J. Springer, M. Vanecek, *Sol. Energy* **77**, 917 (2004)